Intrusive Geometries and Cenozoic Stress History of the Northern Part of the Bohemian Massif

Jiří ADAMOVIČ and Miroslav COUBAL

Institute of Geology, Academy of Sciences of the Czech Republic, Rozvojová 135, 165 02 Praha 6, Czech Republic

ABSTRACT: During its Cenozoic history, the Bohemian Massif (BM) located in the foreland of the Alpine Orogen was subjected to a series of regional intraplate stresses of different parameters. This article combines the former results of paleostress analysis with the analysis of geometries of K/Ar-dated intrusive bodies (77–9 Ma, n = 78) in order to refine the paleostress time scale for the northern part of the BM.

The mechanical model of magma emplacement into an elastic host rock formulated by Pollard (1973) was used as a basis for the determination of the direction of maximum principal stress component from the intrusion shape in horizontal cross section.

Compressional phase α_1 (Senonian) was associated with large-scale ductile deformations while the younger phase α_2 of NE–SW compression with reverse faulting and emplacement of dykes of the pre-rift series (Campanian–L.Eocene) SW of the Lužice Fault. The U.Eocene–M.Miocene extension-dominated period gave rise to the subsymmetrical structure of the Ohře Rift and subsequent graben formation. Uneven areal distribution of intrusive bodies indicative of rift-related N–S extension evidences progressive eastward spread of the rift. Paleostress phase β_1 of E–W to NE–SW extension was effective in the eastern part of the Ohře Rift and adjacent areas of the Bohemian Massif in the interval of 40–26 Ma. Phase β_2 of N–S extension, probably representing an autonomous stress regime of the Ohře Rift dominated at 34–24 Ma (central part) or 26–24 Ma (eastern part). Phase β_3 of approx. NW–SE extension with an increasing intensity between 24 and ?16 Ma resulted in the formation of the present fault-confined graben.

KEY WORDS: intrusive geometries, paleostress, Cenozoic, Bohemian Massif

Introduction

Evolution of regional stress in intraplate settings has a considerable bearing on tectonic deformations, sedimentary basin formation and destruction, magmatic processes and migration of mineralizing fluids, surface processes of erosion and accumulation. *Paleostress analysis* of brittle deformations allows to determine the orientations and relative magnitudes of the principal components of regional stress, i.e. the characteristics and succession (relative ages) of the individual paleostress fields. The effects of any of these phases can be subsequently identified. Timing of the individual phases is constrained mostly geologically: deformations linked with a particular tectonic phase are considered younger than the rocks deformed. Constraints by minerals or rocks filling tectonic structures can be used on condition that their ages and relations to tectonic movements of the given phase are known. Especially the identification of young tectonic phases is highly demanded as the youngest deformations are potentially hazardous for certain construction activities (dams, nuclear power plants and nuclear waste repositories, etc.).

The intensity of magmatic activity and the character of regional stress field are probably interrelated. As the opening of existing ruptures under compressional or transpressional conditions is much less probable than under tensional or transtensional conditions, minima of magmatic activity are generally linked with periods of crustal compression. According to the model of emplacement mechanism based on the assumption of elastic properties of the host rock (Pollard 1973), geometries of intrusive bodies reflect (besides physical parameters of the ascending magma and the host rock) stress field conditions from the time of their emplacement. An analysis of the geometries (in a horizontal cross section) of bodies of known ages should, therefore, allow to infer stress field history for a given region. The present article is an attempt to combine the former results of paleostress analysis with the *analysis of geometries of radiometrically dated intrusive bodies* in order to refine the paleostress time scale for the northern part of the Bohemian Massif.

Structural framework of the northern part of the Bohemian Massif

The Bohemian Massif (BM) is one of the largest European exposures of the Variscan Orogen, consisting of a number of amalgamated terranes of various sizes. These are formed by complexes of Proterozoic to Lower Paleozoic medium- to high-grade metamorphosed rocks, bounded by early Variscan low- to medium-grade metamorphosed volcanosedimentary complexes and late Variscan plutonites at terrane boundaries. The main Variscan deformational event in the northern BM dates to the Famennian–Lower Carboniferous when the Saxothuringian terrane accreted onto the Moldanubian lithospheric block (Oczlon 1992) along a front now broadly arched to the north.

Cenozoic tectonomagmatic history of the BM is similar to that of other Variscan massifs in central and western Europe (Ziegler 1982, 1987). Some of it can be revealed combining field observations with *paleostress analysis*, which employs kinematic indicators on regional and minor fault planes and in their immediate vicinity to identify principal paleostress components (Angelier et al. 1982; Angelier in Hancock ed. 1994). Information on the Cenozoic paleostress history obtained from field mapping and paleostress analysis of shear faults in different areas of northern BM (Schulmann in Jiránek et al. 1989; Coubal 1989, 1990; Coubal and Klein 1992) allowed to recognize phases α_{1-2}, γ and δ of crustal compression and phases β_{1-3} and ε characterized by crustal extension (classification of phases after Coubal 1989).

The period of late Cretaceous rifting in the Alpine foreland allowed the formation of, and subsidence in, the transtensional Bohemian Cretaceous Basin (Uličný 1997) where preserved thicknesses of Cenomanian–Santonian sediments locally exceed 1,000 m. The Sub-Hercynian tectonic inversion in the Alps

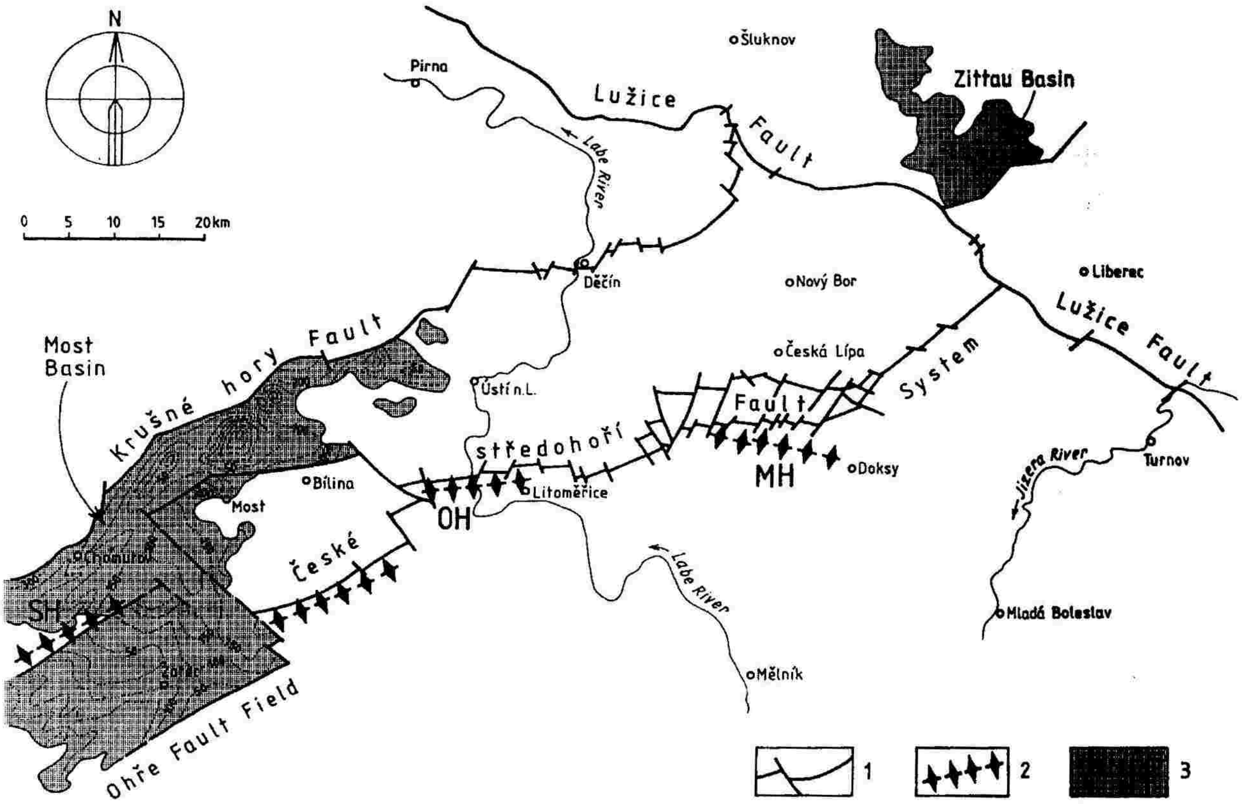

Fig. 1. A sketch of the Ohře Rift graben with limits of the Most Basin and Zittau Basin. 1 – faults; 2 – axes of horst structures, SH – Střezov Horst, OH – Oparno Horst, MH – Maršovice Horst; 3 – base of the Miocene sediments (metres a.s.l.).

marked the end of deposition in this basin in the Santonian and a partial destruction of its northern margin. Crustal compression lasting till the Eocene was responsible for large-scale reverse faulting and ductile deformation in the BM.

Pre-Oligocene tectonic deformations of sediments of the Bohemian Cretaceous Basin, preceding the deposition of the Střezov and Most formations in the Most Basin, indicate two compressional phases: α_1 and α_2.

The effects of the pre-Oligocene compressions are well visible in the Lužice Fault area. A NNE–SSW compression (herein referred to as α_2) resulted in brittle deformations of several generations and culminated by reverse movements with the northern block being uplifted by ca. 1,000 m (Coubal 1990). The age of the reverse movements on the Lužice Fault is constrained by sediments of the Zittau Basin (U.Eocene–L.Miocene) which directly overlie the crystalline basement of the uplifted northern block. Large-scale reverse movements occurred also on the Franconian Fault Zone bounding the BM in the SW (Schröder 1987, Zulauf and Duyster 1997) and on a number of subparallel, NE-dipping faults within the BM (Malkovský 1977, 1987; Coubal 1990).

An E–W-trending anticlinal structure (Kozly Anticline) was formed between Chomutov and Česká Lípa in an axial position relative to the later graben, following the northern boundary of the Central Bohemian Late Paleozoic basins (cf. Coubal and Klein 1992). Also the tectonic style of the East Bohemian folds in NE Bohemia combined with reverse or possibly strike-slip faulting indicates that the formation of these structures resulted from an intensive, approx. NE–SW orientated compression (herein referred to as α_1). As indicated by the destruction of one of these folds (Koberovy Flexure) in the area of Kozákov Hill E of Turnov by reverse movements on the Lužice Fault, phase α_2 is younger than α_1 (Coubal 1989). Other evidence for the pre-Oligocene compressions was found in the Ohře Fault Field, where individual blocks were uplifted along reverse faults which resulted in the erosion of the whole thickness of Cretaceous sediments (Malecha 1961).

An extensive rift system associated with alkaline volcanism and including the Ohře Rift in the BM developed in the Alpine foreland during the Paleogene and some of its grabens actively subside till the present. The course of the Ohře Rift, running ENE–WSW, roughly coincides with the western limb of the Saxothuringian/Moldanubian collisional zone. The Ohře Rift graben (also, Eger Graben) is bounded by the České středohoří Fault Zone in the S and the Krušné hory (Erzgebirge) Fault in the N, both displaying vertical normal displacement of 400–600 m (Fig. 1).

The north Bohemian region began to subside in the Upper Eocene (paleontologically dated sediments of the Staré Sedlo Formation). Incipient graben formation created accommodation space for the deposition of the Střezov Formation (Oligocene) and Most Formation (Lower Miocene). In this period, rift evolution was mostly represented by continuous subsidence with only insignificant movements along faults. Relative subsidence of the graben at its southern margin can be estimated at max. 80 m during the Střezov Fm. deposition and 60–140 m during the Most Fm. deposition. Three tensional phases (β_1–β_3) were recognized (Fig. 2) but their definition was hitherto impossible as paleostress parameters were imperfectly known. N–S extension was identified in the Česká Lípa area and along the Lužice Fault (Coubal and Klein 1992; Coubal 1989).

A post-Lower Miocene uplift of the whole northern BM is

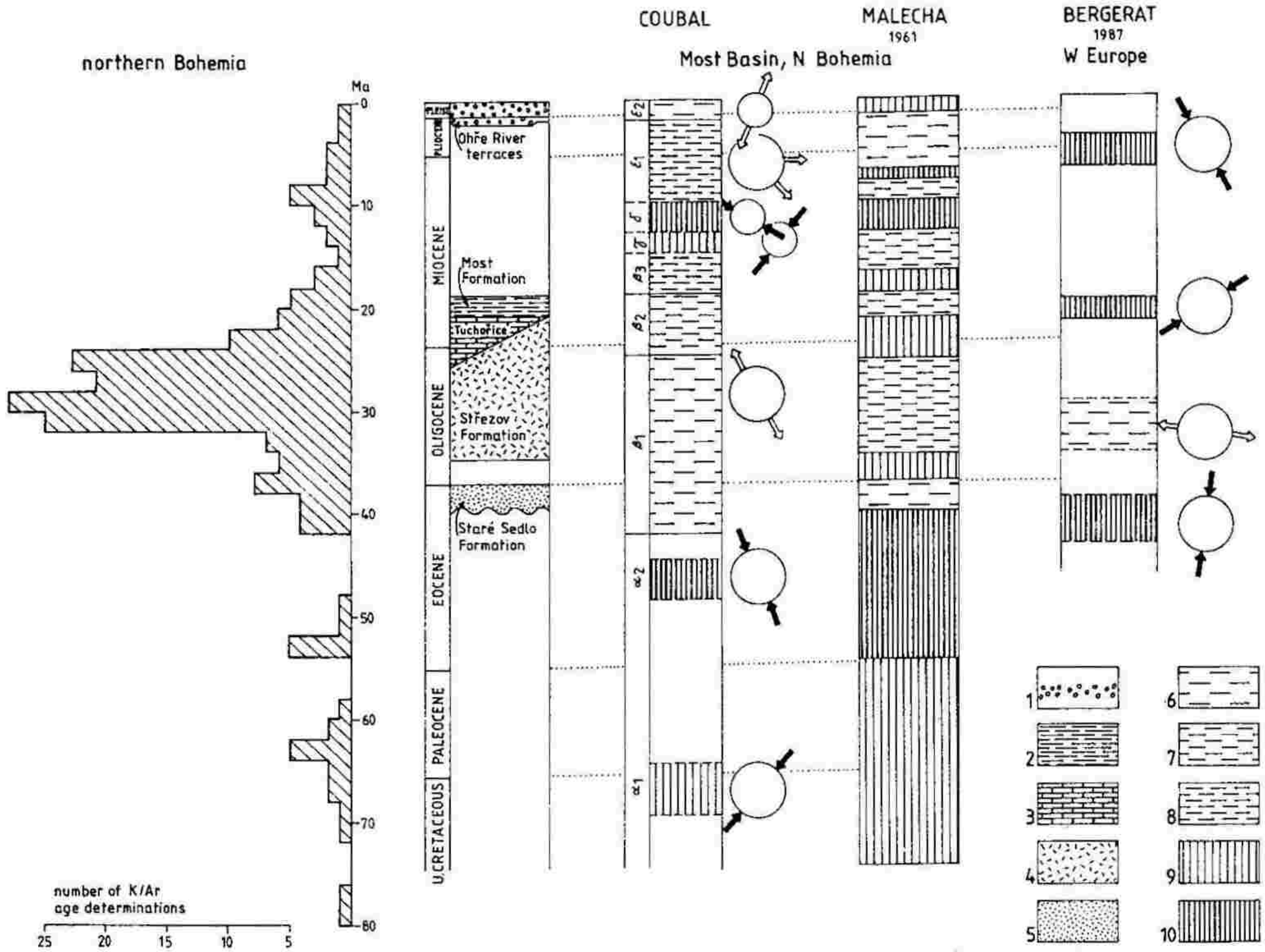

Fig. 2. Stratigraphic column of the Most Basin (centre) with Cenozoic paleostress fields based on paleostress analysis of shear faults in the Most Basin area and western Europe (right) and a histogram showing numbers of K/Ar age determinations of intrusive and volcanic bodies in N Bohemia (left, n = 190). Column headed by COUBAL summarizes results of three unpublished studies by this author from 1991–1992. 1 – sands and gravels; 2 – clay-dominated sediments; 3 – limestones; 4 – volcanic and volcanosedimentary rocks; 5 – sands and clays; 6 – extension, low intensity; 7 – extension, medium intensity; 8 – extension, high intensity; 9 – compression, low intensity; 10 – compression, high intensity.

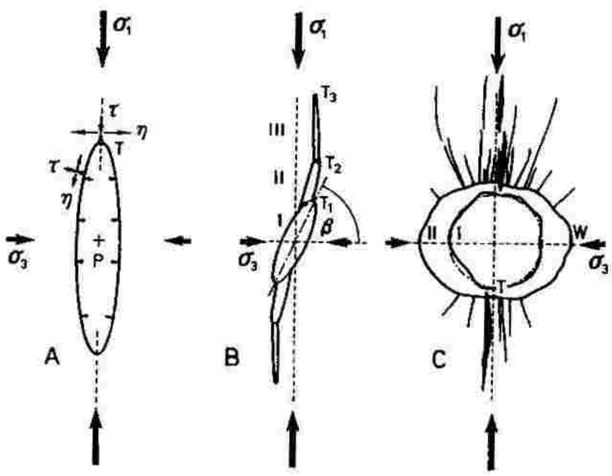

Fig. 3. **A.** Stress distribution around a dyke synaxial with regional stress; p – magma pressure; σ_1 (σ_3) – maximum (minimum) principal component of regional stress; η – tangential stress component acting on dyke at the point studied; τ – normal stress component; T – point on dyke wall where η reaches its maximum value. **B.** Propagation of a dyke orientated oblique to regional stress; β – angle between long axis of dyke contour and minimum principal component of regional stress; I – III stages of dyke propagation. **C.** Geometry and fracturing of a plug growing under inhomogeneous regional stress field; W – points at the contact where η reaches its minimum value.

evidenced by the different altitudes of Neogene sediments preserved in the northern BM and those in Upper Lusatia. Normal movements with a displacement of >600 m occurred along marginal faults of the graben in the M.Miocene (phase β_3). The axial anticlinal structure formed during phase α_1 was destructed to form the Maršovice Horst in the east, the Oparno Horst in the centre and the Střezov Horst in the west (Fig. 1). Blocks north of the Lužice Fault zone subsided (Zittau Basin) and simultaneous subsidence of southern blocks along southerly-dipping splay faults produced a narrow horst.

Two compressional phases, γ and δ, possibly Middle to Upper Miocene in age, can be distinguished in northern Bohemia. Their mutual relationships and timing are difficult to assess as no deposition is documented in this interval. However, superposition of compressional structures on tensional structures of phase β and bodies of neovolcanites indicate that this is a separate group of paleostress fields, considerably younger than compressional phases α_1–α_2. A more precise timing of phases γ and δ can be estimated on the basis of geological setting in the Most Basin only, where Lower Miocene sediments are deformed by slickensides reactivated during these phases. Tensional phase ε post-dating the Upper Miocene compression is evidenced by normal faulting of Pliocene fluvial sediments in the Most Basin. The timing of this phase probably corresponds to the period of volcanic activity along the Lužice Fault in NE Bohemia, i.e. the younger rift series.

In the northern part of the BM, volcanic products ranging from Late Cretaceous to Pliocene in age are preserved in different forms according to their relation to major faults and subsidence histories of the individual tectonic blocks inside and outside the graben (Ulrych and Pivec 1997). Dykes of olivine melilitite – olivine nephelinite clearly preceding rifting (K/Ar ages of 79–48.7 Ma) are referred to as the *pre-rift series*. They are mostly confined to deeply eroded blocks outside the graben. Intrusive and effusive volcanics of the bimodal basanite/olivine nephelinite – trachyte/phonolite *older rift series* (41.9–13 Ma) occur inside as well as outside (only intrusions) the graben. Peak magmatic activity (measured by frequencies of radiometric datings) occurred in the Middle to Upper Oligocene, between 32 and 24 Ma – see Fig. 2. Intrusions and lava flows of picrobasaltic rocks of the *younger rift series* (11.4–3.95 Ma) are areally restricted to the Lužice Fault and the northern reach of the České středohoří Fault.

Paleostress analysis based on geometries of intrusive bodies

Emplacement of intrusive volcanic bodies into the rocks of the Earth's crust (herein referred to as host rocks) can be mediated by different mechanisms. These were subdivided by Noble (1952) into forcible and non-forcible mechanisms. Non-forcible emplacement is typically linked with chemical attack, partial melting (anatexis) or mechanical erosion of the host rock by ascending magma. Bodies thus generated do not give clues to the mechanical parameters of emplacement.

However, in many intrusive volcanic bodies, pathways for the ascending magma were opened by the pressure of magma. A physical model of magma emplacement was formulated by Pollard (1973). In this model, the body is represented by a tube, elliptical in cross section, hosted by a rock considered to be elastic. Any shape of its cross section can be selected from circular to extremely elliptical. The tube is 1. filled with a liquid of hydrostatic (magmatic) pressure p and 2. affected by external regional stress – a combination of lithostatic pressure and tectonic stress. Regional stress is defined by the principal components σ_1 and σ_3. In this paper, positive values are conventionally used for compression and negative values for extension (in accordance with Pollard 1973). The problem is solved as a 2-D one in a plane perpendicular to the tube length.

The elastic model assumes an infinitely thin fracture at the beginning of the emplacement, which was penetrated by magma. As the magnitude of magma pressure exceeded that of regional stress, the fracture dilated. The difference between magma pressure and regional stress is defined as driving pressure. Possible variations in the magnitude of driving pressure could have resulted in variations in intrusive geometries. Eventually,

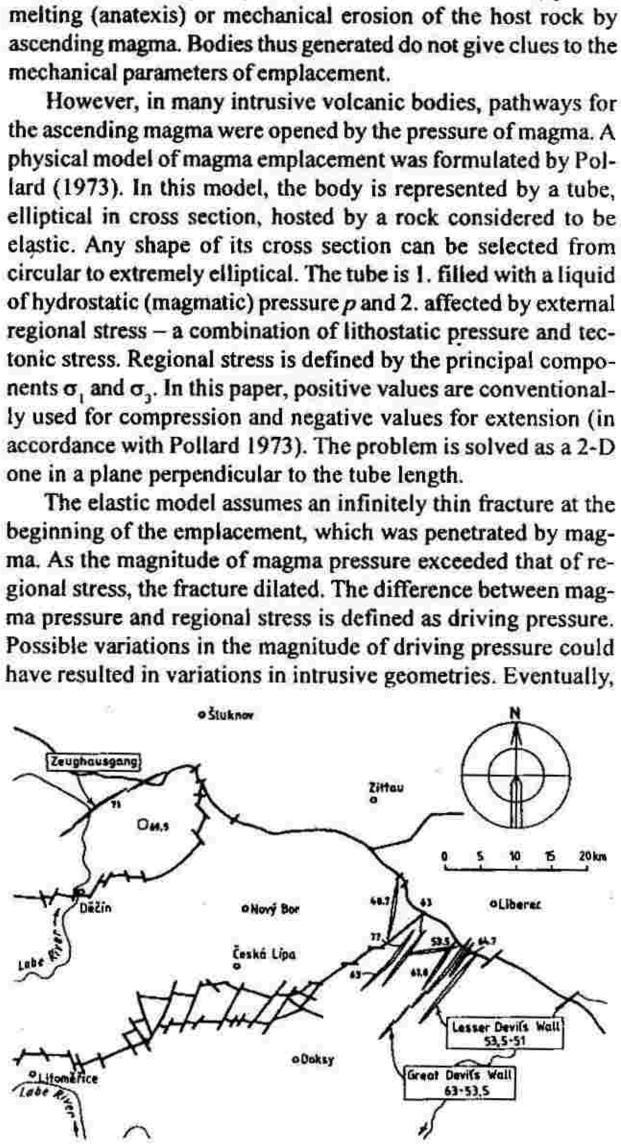

Fig. 4. Geometries of intrusive bodies, pre-rift series (79–48.7 Ma, n = 11). Contours of bodies not to scale. Ages in Ma. Radiometric ages adopted from Kopecký (1987–1988), Pfeiffer 1994, Pivec et al. (1998), Shrbený (1988) and Shrbený and Vokurka (1985).

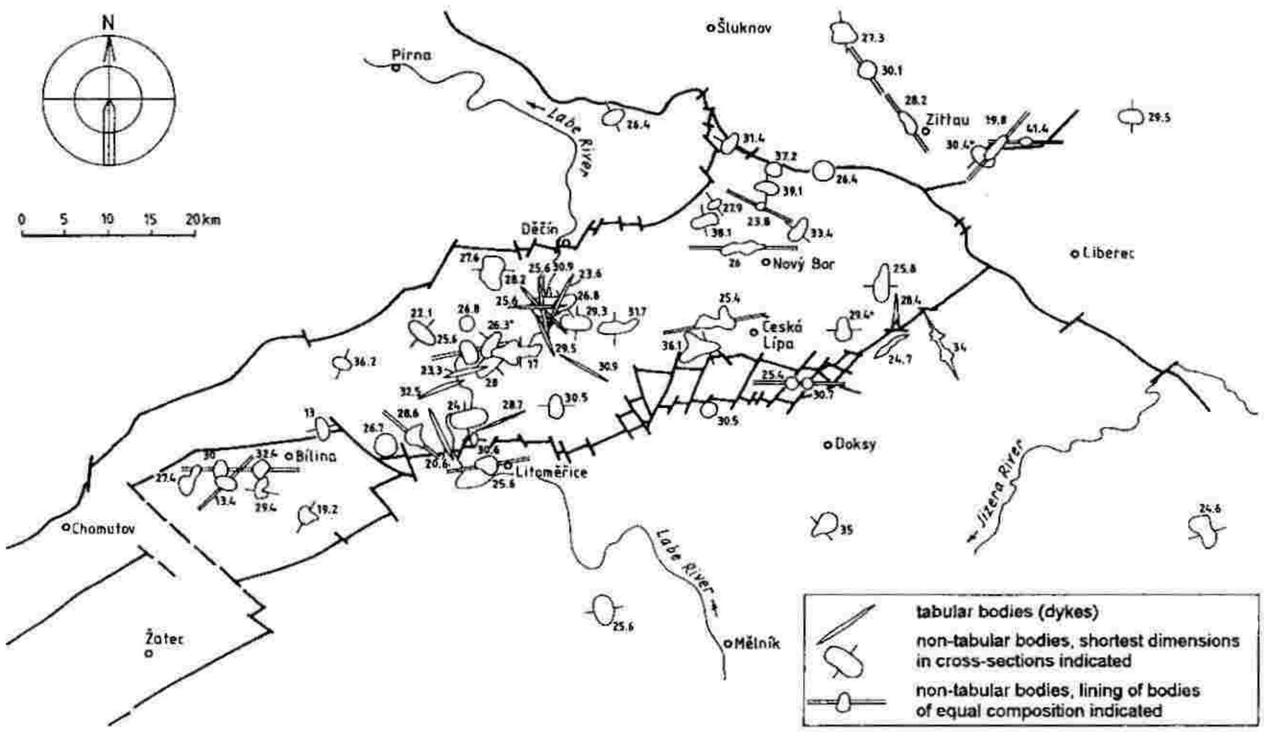

Fig. 5. Geometries of intrusive (volcanic) bodies with indicated linear elements, older rift series (41.9–13 Ma, n = 65). Contours of bodies not to scale. Ages in Ma, those marked with a cross represent means of two or more measurements. Radiometric ages adopted from Alibert et al. (1987), Cajz et al. (this volume), Kaiser and Pilot (1986), Kopecký (1987–1988), Pfeiffer et al. (1984), Pivec et al. (1998), Shrbený (1969, 1988), Shrbený and Vokurka (1985), Vokurka et al. (1992) and Wilson et al. (1994).

magma pressure equilibrated with the regional stress in the host rock, magma got inhibited in its movement and solidified. The present geometries of intrusive bodies result from this equilibrated stress field, thus giving evidence of the effects of both the magma pressure and regional stress (Pollard et al. 1975; Delaney and Pollard 1981).

Dykes

In the model of Pollard (1973), tabular bodies – sheet intrusions (i.e. dykes) are defined as intrusive bodies with a length/width ratio > 10 whereas non-tabular bodies (plugs and stocks) as those with a length/width ratio < 10 in cross section.

Magma pressure p inside the dyke and regional stress σ acting over an infinite distance combine to form stress in the host rock. At any point in the host rock, this stress can be decomposed into two components: τ acting normal to dyke contact and η acting tangential to dyke contact (Fig. 3A). If β= 90° (Anderson's presumption), the highest tangential stress originates directly at dyke terminations (point T) and the dyke propagates in the original direction. Magnitudes of components τ and η at point T can be expressed by equations (adapted from Pollard 1973):

$$\eta = p + \sigma_3 - \sigma_1 + (\sigma_3 - p) \,.\, 2 \,.\, l/t \quad (1)$$

$$\tau = p \quad (2)$$

where η is tangential stress, τ is normal stress, σ_1 (σ_3) is maximum (minimum) component of regional stress, p is magma pressure, l is dyke length and t is dyke thickness.

Figure 3A implies that tangential stress tends to break the outer contact of the body. Magnitude of the stress depends on the curvature radius of the contact. If the l/t ratio of the intrusion is high (as in dykes), an extremely high tangential stress is concentrated at dyke terminations (point T). Such stress may exceed the tensile strength of the host rock even at low values of magma pressure thereby allowing dyke propagation.

If the minimum component of regional stress is not normal to dyke walls (β different from 90°, Fig. 3B), the maximum tangential stress is concentrated at a point different from T and the direction of further dyke propagation tends to be close to the Anderson's presumption.

Isometric bodies

Fig. 3C, contour I, shows a horizontal section across a plug or a stock (a pipelike, non-tabular body of circular cross section) where magma pressure increases. External regional stress is described using two principal components. The fact that the principal components of regional stress are of different magnitudes indicates a considerable influence of tectonic stress. As long as magma pressure exceeds both principal components of regional stress, the plug is dilated and becomes slightly elliptical in cross section with the longest axis parallel to the minimum principal component of regional stress (Fig. 3C, contour II). During further stages of dilation, tangential stress at the contact increases and its minimum value (i.e., the maximum extension) is always reached at point W. If the magma pressure is sufficiently high, tensile strength of the host rock is exceeded at point T and fractures normal to the plane of the contact are formed (Fig. 3C). These fractures effectively facilitate the body to propagate along fracture planes, i.e. normal to the direction of its present elongation and parallel to the maximum principal component of regional stress σ_1. Further dilation may lead to the transformation of the original plug/stock into a dyke.

The mechanism of elastic dilation in large-diameter plugs is probably of limited effect. Elastic dilation of the body must be compensated by compression of host rocks while compressibility of rocks is generally low. If elastic mechanism is the only mechanism involved in plug formation, dilation magnitudes of plugs should be equal to their radii. However, radii of plugs commonly exceed several hundreds of metres. The origin of such bodies must have involved other mechanisms besides elastic dilation.

The situation is different in dykes where the maximum dilation occurs at their midpoint and reaches 50% of dyke thickness. With the maximum thicknesses of mafic dykes being several metres, the dilation can be considered small enough to be fully compensated by compression of ambient host rock.

Radial dykes and lateral intrusions around plugs and stocks

Radial fractures around plugs and stocks (Fig. 3C) are frequently filled with magma penetrating laterally from the central plug thus forming radial dykes. Studies of Recent volcanoes by Nakamura (1977) have shown that lateral craters (intrusions) of large polygenetic volcanoes are often arranged into linear swarms and probably represent finger-like extensions of growing radial dykes (cf. Pollard et al. 1975). Similarly, also plugs of similar petrographic composition showing linear arrangement should represent frontally prograding extensions of more deeply located tabular intrusions (Kopecký 1974). Radial dykes as well as lateral intrusions are generally monogenetic bodies, whose shape and orientation are connected with a single major volcanic event.

An ideal radial arrangement of dykes and their even distribution around the central plug of roughly circular cross section indicate that the two horizontal principal components of regional stress were either of the same magnitude in the time of emplacement or their magnitudes were small relative to magma pressure. This is the case where regional stress is represented only by lithostatic pressure.

A centrally non-symmetrical stress field is produced around the plug if the two principal components of regional stress in horizontal plane differ from each other in their magnitudes, being comparable to that of magma pressure. The distribution of radial dykes (Fig. 3C) is not perfectly symmetrical, reflecting the orientation of regional stress. Maximum density of radial dykes and fractures is observed to the direction of maximum principal component of regional stress from the centre of the plug. These ruptures also display the highest lengths of all. In other directions, the contact of the plug is intersected by a sparser system of mostly shorter fractures and dykes with their planes tending to further propagate parallel to a plane normal to minimum principal component of regional stress (Nakamura 1977). The arrangement of radial dykes, lateral intrusions and radial fractures in the periphery of a plug can be considered a good indicator of paleostress orientation in the time of volcanic activity.

Paleostress determination

According to the above model, there are several simple criteria for the determination of orientations of principal paleostress components based on their shape in cross section: minimum principal component of paleostress (σ_3) was lying in a horizontal plane and, at the same time, 1. normal to straight dyke walls or parallel dyke swarms, 2. normal to terminations of sigmoidal dykes, 3. parallel to elongation axis of plugs with subisometric cross sections and, at the same time, normal to the most frequent strike of associated radial dykes, 4. normal to lines of plugs of similar petrographic composition or lines of arrangement of lateral intrusions of polygenetic volcanoes.

Data processing

Some of the oldest radiometric datings come from the K/Ar Laboratory of the Czech Geological Survey, which has been in operation since late 1960s. These data were summarized in an unpublished study by Shrbený and Vokurka (1985) and the information by Shrbený (1988). Other data used in this study come from the Laboratoire de Petrographie-Volcanologie de l'Université de Paris in Orsay (Bellon and Kopecký 1977, see Kopecký 1987–1988), the IGEM Laboratory in Moscow (M. M. Arakelyanc, see Kopecký 1987–1988) and the Radievyi Institut imeni Khlopina in St. Petersburg, Russia (E. Anderson, see Pivec et al. 1998), the Bergakademie Freiberg (Pfeiffer et al. 1984; Kaiser and Pilot 1986), the University of Leeds (M. Wilson, see Wilson et al. 1994) and the Institute of Nuclear Research of the Hungarian Academy of Sciences (ATOMKI) in Debrecen (K. Balogh in Cajz et al., this volume). As different constants were previously used for calculations, former ages produced by the laboratories of CGS in Prague and IGEM in Moscow were corrected using the formula:

$$\text{Age (Ma)} = 0.9577 \times \text{Age}_{\text{original}}\ \text{(Ma)} + 0.0790 \qquad (3)$$

proposed by Shrbený and Vokurka (1985). Sources of K/Ar ages of volcanic rocks used for the herein presented paleostress reconstruction are also cited in captions to Figs. 4 and 5.

In the first step, 190 existing $^{40}K/^{40}Ar$ datings (14 younger-, 153 older-, 23 pre-rift series) of 152 bodies (10 younger-, 128 older-, 14 pre-rift series) were considered from northern BM: the České středohoří Mts. and Most Basin (Tertiary), Krušné hory Mts., Lusatia, Saxony, and from the adjacent part of the Bohemian Cretaceous Basin – see histogram in Fig. 2. Then, bodies other than dykes or plugs (i.e., isolated lava sheets, sills, lopoliths etc.) and bodies of dubious forms were eliminated from the data set. Where different ages were obtained for the same body by different laboratories, the most recently published age was always taken into account. Only those intrusive bodies were studied whose shapes in horizontal cross section were well documented in geological maps at scales 1:100,000 or larger. This way, 78 intrusions of (sub)volcanic rocks were selected.

The following maps were used: Müller (1933), Chaloupský (1988), Tyráček et al. (1988), Lobst (1993), Cajz ed. (1996), Valečka ed. (1996), Steding (1998), 11 sheets of geological maps 1:50,000 published by the Czech Geological Survey and the schematic map in Alibert et al. (1987).

A *linear element* was found for each of the bodies and measured from the geological map, characterizing the direction of maximum principal component of regional stress σ_1 (maximum compression) in horizontal plane, as inferred from the model above. Linear elements are:

- in tabular bodies (dykes, length/width ratio >10), parallel to the elongation (strike) of the body;
- in non-tabular bodies (length/width ratio < 10), perpendicular to the elongation of the body;
- parallel to linear arrangement of bodies of the same composition.

Linear elements and contours of all studied bodies were plotted into a map separately for the pre-rift series (Fig. 4) and older rift series (Fig. 5) to show regional variations in paleostress and its relation to major faults. No map was drawn for the younger rift series as most of these bodies are relicts of surficial lava flows.

Intrusive geometries of the pre-rift series (79–48.7 Ma, n = 11)

Dykes and dyke swarms of the pre-rift series are independent of the later rift structure. In contrast, they are concentrated in the area of the Lužice Fault, being generally restricted to its footwall (southwestern) block. Intersections of these dykes with the Lužice Fault are hidden beneath Pleistocene colluvial sediments. Discrete, small intrusions NE of the Lužice Fault show no clear relationship with these dykes. The oldest body of the pre-rift series exposed on the surface is the dyke of micromelilitolite at Děvín Hill near Hamr (77 Ma, Pivec et al. 1998), the youngest body is the dyke of olivine melilitite at Buková Hill near Jablonné (48.7 ± 7.4 Ma, Shrbený 1988). The body of nepheline olivine melilitite at Vyhlídka Hill near Jetřichovice (69.5 ± 10.5 Ma, Shrbený 1988) shows no elongation. Directions of linear elements (Fig. 4) are relatively uniform, ranging between 35–57°, with the exception of the youngest dykes.

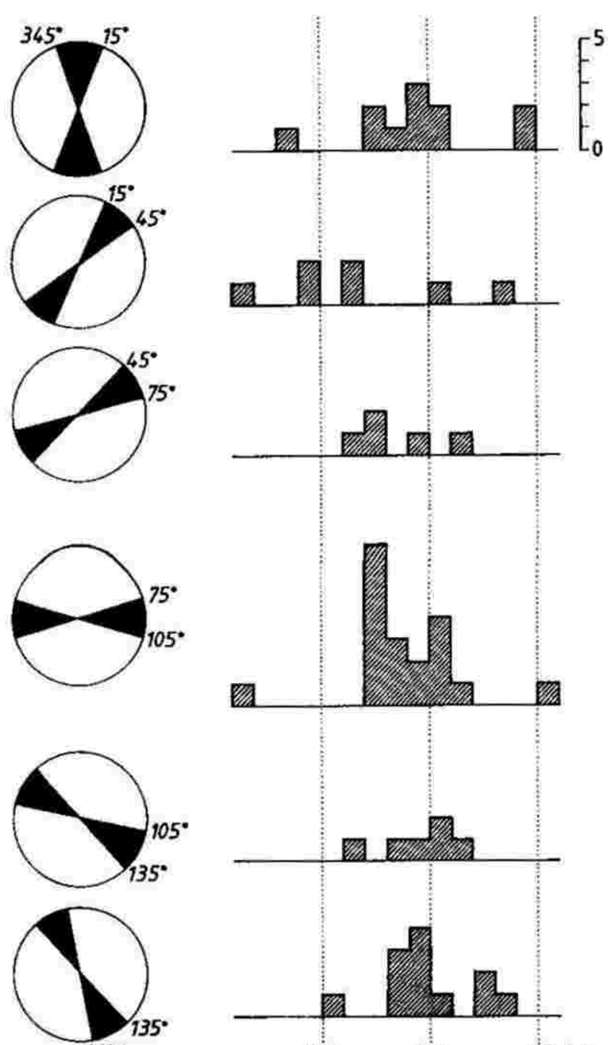

Fig. 6. Histograms of linear element directions for intrusive (volcanic) bodies, older rift series (41.9–13 Ma, n = 60). Numbers of bodies are indicated on vertical axis, K/Ar ages in 2 m.y.-intervals on horizontal axis.

Intrusive geometries of the older rift series (41.9–13 Ma, n = 65)

Emplacement of bodies of the older rift series was roughly contemporaneous with the long period of crustal extension (phases β_1–β_3). As the oldest body of this series (olivine basaltoid at Všechlapy near Teplice) is probably a relict of an isolated lava flow (V.Cajz, pers. comm.), the oldest occurrence included in this study are the E–W-lined effusions of olivine nephelinite near Bogatynia (41.4 ± 1.2 Ma, Alibert et al. 1987). The youngest body is the plug of olivine basalt at Pohradická hora Hill near Bílina (13 ± 1.1 Ma, Cajz et al. this volume). Out of the total of 65, five bodies showed no elongation.

Variations in linear element directions (thus also paleostress field characteristics) in space and time across the northern part of the BM can be identified from data in Fig. 5, pointing to different paleostress histories for the eastern part of the České středohoří Mts. (CS) with Lusatia (east of line Děčín–Mělník) and the western part of the CS.

Bodies with N–S to NW–SE linear element directions (135° to 195°), mostly of trachytic composition, are considerably more frequent in the east: 95% of these bodies from the interval of 40–26 Ma lie east of the above mentioned line. Here, bodies with subequatorial linear element directions (45° to 105°) become dominant as late as in the 26–24 Ma interval. In contrast, the western part of the CS is characterized by emplacement of bodies of subequatorial linear elements during the whole interval of 34–24 Ma.

Histograms of linear element directions for intrusive (volcanic) bodies of different ages are shown in Fig. 6. 2 m.y.-intervals were chosen as optimum with respect to the number of data and their generally low precision.

The period **before 34 Ma** is almost devoid of any subequatorial elements, thus indicating approx. N–S maximum principal stress. With the exception of Zámecký vrch Hill in Teplice (36.2 ± 5.5 Ma), all bodies of this age lie in the eastern CS and Lusatia. These trachytic or phonolitic plugs lie inside the present graben – Břidličný vrch Hill (38.1 ± 5.9 Ma) and Velká Tisová Hill (39.1 ± 6 Ma, all data from Shrbený 1988) in the Nový Bor area – and outside the graben – Vrátenská hora Hill (35 Ma, Vokurka et al. 1992). Isometric phonolite plug of Jedlová Hill (37.2 ± 5.7 Ma, Shrbený 1988) lies very close to the Lužice Fault. Basanite dyke of Malý Jelení vrch Hill (34 Ma, Pivec et al. 1998) is associated with the northern reach of the České středohoří Fault.

The interval of maximum frequencies of radiometric datings of **34–24 Ma** contains two maxima of subequatorial elements: 32–30 Ma and 26–24 Ma, indicating two peaks of subequatorial maximum principal stress. Bodies of the older peak lie mostly in the western part of the CS, being associated with the České středohoří Fault Zone, e.g. phonolitic and trachytic plugs Špičák Hill and Želenický vrch Hill W of Bílina (30 ± 1.1 Ma – Kaiser and Pilot 1986 and 32.4 Ma – Kopecký 1987–1988) and Kalich Hill E of Litoměřice (30.5 ± 4.6 Ma, Shrbený 1988). In contrast, bodies of the younger peak are evenly distributed across the graben, being more frequent in its axial part, e.g. the trachytic plug of Mariánská skála Hill in Ústí nad Labem (25.6 Ma, Kaiser and Pilot 1986) and numerous basanitic bodies dated by Wilson (Wilson et al. 1994).

The period of 30–26 Ma is dominated by bodies with N–S to NW–SE linear element directions. They are concentrated mostly in the Roztoky Intrusive Centre of the České středohoří Mts. S of Děčín and the Lužice Fault area (see Fig. 5). The wide distribution of these bodies in the eastern CS and Lusatia may partly result from reopening of pre-existing ruptures formed during the period of 40–34 Ma. Phonolitic bodies of this age are arranged into approx. NW–SE-trending lines W of Zittau (Pfeiffer et al. 1984, Kaiser and Pilot 1986 and the map of Steding 1998), possibly resulting from magma emplacement along splays to the Lužice Fault. A large composite volcano with products of mostly tephritic composition developed in the central part of the CS in this period (Cajz et al., this volume).

The period **after 24 Ma** is, in analogy with the period of 40–34 Ma, characterized by low number of bodies with subequatorial linear elements and the few dated intrusive bodies rather indicate a NE–SW maximum principal stress. These include, e.g., basanite and nephelinite intrusions between Litoměřice and Ústí nad Labem (Wilson et al. 1994), a plug of trachybasalt at Střížovice (22.1 Ma, Kopecký 1987–1988), a phonolite plug at Olešnice (17 ± 0.9 Ma, Shrbený 1969) near Ústí nad Labem and fault-confined basanite extrusions near Zittau (Alibert et al. 1987).

Intrusive geometries of the younger rift series (11.4–3.95 Ma)

Most of these bodies are relicts of surficial lava flows whose shapes in the section of the present surface do not reflect paleostress conditions. These extrusions are mostly associated with the NW–SE-striking Lužice Fault. The only two dated intrusive bodies (dyke systems) of Útěchovický Špičák Hill and Havraní návrší Hill (9 Ma, Ulrych and Pivec 1997), located close to the intersection of the České středohoří Fault with the Lužice Fault, show complex geometries dominated by E–W-striking dykes.

Discussion

First, it has to be stressed that the radiometric datings used come from different laboratories and that some of the analyses are of low accuracy (Shrbený and Vokurka 1985). Therefore, their correlation must be done with caution. However, the consistency of data and their compatibility with results from paleostress analysis of brittle structures clearly show that the pre-rift series corresponds to phases α_1–α_2 and the older rift series to phases β_1–β_3.

Intrusive geometries of bodies of the **pre-rift series** older than ca. 50 Ma indicate a NE–SW orientation of maximum principal stress component σ_1. The study of brittle structures in the Lužice Fault Zone (Coubal 1990) has shown that the series of transverse, NE–SW-striking ruptures in the footwall block probably controlling the dyke emplacement was associated with α_2-thrusting along the fault zone and that this thrusting was, in turn, driven by NE–SW crustal compression. This implies that the emplacement of dykes of the pre-rift series was coeval with or only slightly younger than the thrusting, both resulting from NE–SW compression. The distribution of dykes of the pre-rift series is a typical example of magma emplacement under compressive stress conditions sensu Nakamura (1977).

Parallelism between the main phase of reverse faulting on the Lužice Fault and the emplacement of dykes of the pre-rift series suggests that the timing of pre-Oligocene compressional phases in the Most Basin area estimated from paleostress analysis of shear faults (Fig. 2) should be revised. Phase α_2 of NE–SW compression in N Bohemia lasted from the late Cretaceous to Lower Eocene; hence, the preceding phase of ductile structure origin (α_1) must be considered late Cretaceous in age. Based on the comparison with the Cenozoic tectonic history of the Alpine foreland (Ziegler 1987; Bergerat 1987; Ziegler et al. 1995) these compressional phases can be paralleled with the Sub-Hercynian and Laramide phases, respectively.

The analysis of intrusive geometries of the **older rift series** can be used to refine the paleostress time scale for the wide β-extension period. The most striking fact is the difference between linear elements in the western vs. eastern part of the studied region. The N–S to NW–SE directions of maximum principal component of regional stress in the eastern CS and Lusatia in the Middle Eocene to Upper Oligocene (40–26 Ma) were probably associated first with the N–S compression at the Eocene/Oligocene boundary compatible with the Pyrenean phase in the Alps (Ziegler 1982, 1987; Bergerat 1987) and later with the E–W extension of tectonic origin, detected in sedimentary basins in the western part of the Alpine foreland (ibid.). The effects of the latter phase, including the opening of the Norwegian-Greenland Sea and Limagne-Bresse-Rhine grabens were dated by the above authors to the Eocene–Middle Miocene. On the other hand, no clear manifestations of these paleostress fields were encountered in the western part of the CS.

Neither the linear elements nor the geographical distribution of intrusive bodies emplaced between 40 Ma and 34 Ma (26 Ma in the eastern CS and Lusatia) were controlled by the Ohře Rift structural plan but rather by regional paleostress field of tectonic origin. This is also supported by the distribution of sediments of the Upper Eocene Staré Sedlo Formation. The first signs of N–S extension appeared at ca. 32.5 Ma as indicated by the age of first bodies with subequatorial elements in the western part of the CS. In the eastern CS and Lusatia, this structural plan was adopted not earlier than at 26 Ma. As the lateral coexistence of two different paleostress fields of regional character seems improbable (cf. Zoback 1992), these results must be considered an evidence for an autonomous paleostress regime of the Ohře Rift and its spread to the east at around 26 Ma.

A sudden decrease in the number of dated intrusive/volcanic bodies after 24 Ma probably reflects a decline in the dynamics of the rift development and marks the beginning of volcanic collapse. The geometries of the few intrusive bodies of this age (see above) are in agreement with geological observations from shear faults, both indicating NW–SE extension across the Lower and Middle Miocene.

The new results have serious implications for the analysis of sedimentary basin formation and filling: deposition of the Střezov Formation in the Most Basin and its equivalent in the Zittau Basin, the Loučeň Formation (Oligocene), must have been controlled by different paleostress fields. It was not until the late Upper Oligocene that the sedimentation in the whole northern BM got under control of rift-related, graben-forming paleostresses: N–S extension (26–24 Ma) and NW–SE extension (24–16 Ma).

Conclusions

The analysis of intrusive geometries, combined with the previous results from paleostress analysis of shear faults, provided a more clear picture of paleostress field history for the northern part of the Bohemian Massif.

Two pre-Oligocene compressional phases were identified: a phase of ductile structure origin α_1 (Senonian) and a younger phase α_2 of NE–SW compression associated with reverse faulting and emplacement of dykes of the pre-rift series (Campanian–L.Eocene) SW of the Lužice Fault. These phases can be paralleled with the Sub-Hercynian and Laramide phases in the Alpine foreland (Ziegler et al. 1995; Bergerat 1987).

The principal result of this study is the subdivision of the long Middle Eocene to Middle Miocene β extension-dominated period. On the basis of the new data, the following regional paleostress fields can be distinguished:

β_1 – paleostress field characterized by E–W to NE–SW extension, effective in the eastern part of the Ohře Rift and adjacent areas of the Bohemian Massif in the interval of 40–26 Ma,

β_2 – paleostress field characterized by N–S extension, associated with the development of the Ohře Rift and progressively spreading from its central part in the Most Basin (onset at 34 Ma) to its eastern part (onset at 26 Ma), and

β_3 – paleostress field characterized by approx. NW–SE extension, commenced at 24 Ma. Its intensity increased in post-Lower Miocene period (after c. 18 Ma) in connection with the tectonic uplift of the northern part of the BM. Large-scale normal movements on major faults marked the formation of the present fault-confined Ohře Rift graben.

No reliable data on intrusive geometries exist from the Upper Miocene to Pleistocene. The minimum frequency of radiometric datings from 16–12 Ma may be associated with Middle to Upper Miocene compressional phases γ and δ inferred from the study of shear faults.

Acknowledgements

The authors wish to thank J. Ulrych and V. Cajz, Institute of Geology AS CR Prague, for their generous help with radiometric data acquisition and for friendly consultations. We also thank A. Špičák, Institute of Geophysics AS CR Prague, for his valuable comments to the manuscript of this paper.

References

ALIBERT C., LETERRIER J., PANASIUK M. and ZIMMERMANN J.L., 1987. Trace and isotope geochemistry of the alkaline Tertiary volcanism in southwestern Poland. *Lithos*, 20, 311–321.

ANGELIER J., TARANTOLA A. and VALETTE B. 1982. Inversion of field data in fault tectonics to obtain the regional stress. *Geophys. J. R. Soc.*, 69, 607–621.

BELLON H. and KOPECKÝ L. 1977. Spectres d'âges radiométriques du volcanisme du rift du Massif bohémien. *5eme Réunion annuelle des sciences de la terre, Rennes, Soc. géol. Fr. éd.*, 57.

BERGERAT F. 1987. Stress fields in the European Platform at the time of Africa-Eurasia collision. *Tectonics*, 5 (2), 99–132.

CAJZ V. ed. 1996. *České středohoří. Geologická a přírodovědná mapa, 1:100 000.* Czech Geological Survey, Praha.

CHALOUPSKÝ J. 1988. *Přehledná geologická mapa Krkonoš a Jizerských hor, 1:100 000.* Czech Geological Survey, Praha.

COUBAL M. 1989. Projevy saxonské tektogeneze v centrální části české křídové pánve. Ph.D. Thesis, Czech Geological Survey Prague.

COUBAL M. 1990. Compression along faults: example from the Bohemian Cretaceous Basin. *Miner. slovaca*, 22, 139–144.

COUBAL M. and KLEIN V. 1992. Development of the Saxonian tectonics in the Česká Lípa region. *Věst. Čes. geol. Úst.*, 61 (1), 25–45.

DELANEY P.T. and POLLARD D.D. 1981. Deformation of host rocks and flow of magma during growth of minette dikes and breccia bearing intrusions near Ship Rock, New Mexico. *U. S. geol. Surv. Prof. Pap.*, 1202.

HANCOCK P.L., ed. 1994. *Continental Deformation.* Pergamon Press, Oxford. 421 pp.

JIRÁNEK J., SCHOVÁNKOVÁ D. and SCHULMANN K. 1989. Stavba tělesa teplického ryolitu. *Sbor. Západočes. Muz. (Plzeň), Přír.*, 1988, 67, 56–62.

KAISER G. and PILOT J. 1986. Weiter K–Ar Datierung an jungen Vulkaniten. *Z. geol. Wiss.*, 14, 121–124.

KOPECKÝ L. 1974. Detection of faults and determination of their order in the regions of platform volcanism. *Sbor. geol. Věd, Geol.*, 26, 167–225.

KOPECKÝ L. 1987–1988. Mladý vulkanismus Českého masívu, I–VI. *Geol. Hydrometal. Uranu*, 11(3), 30–67; 11(4), 3–44; 12(1), 3–40; 12(2), 3–56; 12(3), 3–40; 12 (4), 3–40.

LOBST R. 1993. *Geologische Karte der Nationalparkregion Sächsische Schweiz 1:50 000.* Sächs. Landesamt f. Umwelt u. Geologie, Freiberg.

MALECHA A. 1961. Příspěvek k saxonské tektonice severozápadní části Českého masivu. *Sbor. Ústř. Úst. geol., Geol.*, 26 (2), 227–296.

MALKOVSKÝ M. 1977. Důležité zlomy platformního pokryvu severní části Českého masívu. *Výzk. Práce Ústř. Úst. geol.*, 14, 1–32.

MALKOVSKÝ M. 1987. The Mesozoic and Tertiary basins of the Bohemian Massif and their evolution. *Tectonophysics*, 137, 31–42.

MÜLLER B. 1933. Erläuterungen zur geologischen Karte des Bezirkes Deutsch-Gabel in Böhmen. *Firgenwald*, 6 (1), 8–85.

NAKAMURA K. 1977. Volcanoes as possible indicators of tectonic stress orientation – principle and proposal. *J. Volcanol. Geotherm. Res.*, 2: 1–16.

NOBLE J.A. 1952. Evaluation of criteria for the forcible intrusion of magma. *J. Geol.*, 60: 34–57.

OCZLON M.S. 1992. Gondwana and Laurussia before and during the Variscan Orogeny in Europe and related areas. *Heidelberger Geowiss. Abh.*, 53: 1–56.

PFEIFFER L., KAISER G. and PILOT J. 1984. K–Ar-Datierung von jungen Vulkaniten im Süden der DDR. *Freib. Forsch.-H., C* 389, 93–97.

PFEIFFER L. 1994. Der tertiäre Magmatismus im Erzgebirge und in den benachbarten Gebieten der Tschechischen Republik. *Eur. J. Mineral.*, Beih. 6, 179–228.

PIVEC E., ULRYCH J., HÖHNDORF A. and RUTŠEK J. 1998. Melilitic rocks from northern Bohemia: geochemistry and mineralogy. *Neu. Jb. Mineral., Abh.*, 173, 119–154.

POLLARD D.D. 1973. Derivation and evaluation of a mechanical model for sheet intrusions. *Tectonophysics*, 19, 233–269.

POLLARD D.D., MULLER O.H. and DOCKSTADER D.R. 1975. The form and growth of fingered sheet intrusions. *Geol. Soc. Am. Bull.*, 86, 351–363.

SCHRÖDER B. 1987. Inversion tectonics along the western margin of the Bohemian Massif. *Tectonophysics*, 137, 93–100.

SHRBENÝ O. 1969. Tertiary magmatic differentiation in the central part of the České středohoří Mountains. *Čas. Mineral. Geol.*, 14 (3–4), 285–298.

SHRBENÝ O. 1988. Stáří neovulkanismu Českého masívu. *Zpr. geol. Výzk. v Roce 1985*, 172–174.

SHRBENÝ O. and VOKURKA K. 1985. *Současný stav geochronologického a izotopického výzkumu neovulkanitů Českého masívu a jejich uzavřenin.* MS Archive Czech Geol. Survey, Praha.

STEDING D. 1998. *Geologische Karte der eiszeitlich bedeckten Gebiete von Sachsen, 1:50 000. Zittau 2770.* Sächs. Landesamt f. Umwelt u. Geologie, Freiberg.

TYRÁČEK J., MALKOVSKÝ M. and SCHOVÁNEK P. 1988. *Přehledná geologická mapa severočeské hnědouhelné pánve a jejího okolí*. Czech Geological Survey, Praha.

ULIČNÝ D. 1997. Sedimentation in a reactivated, intracontinental, strike-slip fault zone: the Bohemian Cretaceous Basin, Central Europe. *18th IAS Regional European Meeting of Sedimentology, Heidelberg, September 2–4, 1997. Abstracts*. 347.

ULRYCH J. and PIVEC E. 1997. Age-related contrasting alkaline volcanic series in North Bohemia. *Chem. Erde*, 57, 311–336.

VALEČKA J. ed. 1996. *České Švýcarsko. Geologická a přírodovědná mapa 1:25 000*. Czech Geological Survey, Praha.

VOKURKA K., BENDL J. and MELKOVÁ A. 1992. Sr isotopes of some trachytes and cognate rocks from northern Bohemia. *Čas. Mineral. Geol.*, 37 (4), 319–323.

WILSON M., ROSENBAUM J. and ULRYCH J. 1994. Cenozoic magmatism of the Ohře rift, Czech Republic: Geochemical signatures and mantle dynamics. *Abstracts, Int. Volcanolog. Congress, Ankara*. 1 p.

ZIEGLER P.A. 1982. *Geological atlas of Western and Central Europe*. Shell Internationale Petroleum Maatschappij B.V., Hague, 130 pp.

ZIEGLER P.A., ed. 1987. Late Cretaceous and Cenozoic intraplate compressional deformations in the Alpine foreland. *Tectonophysics*, 137, 389–420.

ZIEGLER P.A., CLOETINGH S. and van WEES J.-D. 1995. Dynamics of intra-plate compressional deformations: the Alpine foreland and other examples. *Tectonophysics*, 252, 7–59.

ZOBACK M.L. 1992. First and second order patterns of stress in the lithosphere: the World Stress Map Project. *J. Geophys. Res.*, 97, 11703–11728.

ZULAUF G. and DUYSTER J. 1997. Supracrustal intraplate thickening of Variscan basement due to Alpine foreland compression: Results from the superdeep well KTB (Bohemian Massif, Germany). *Tectonics*, 16 (5), 730–743.